Comparing the Tsallis distribution with and without thermodynamical description in p+p collisions

H. Zheng[1*] and Lilin Zhu[2†]
[1] *Laboratori Nazionali del Sud, INFN, via Santa Sofia, 62, 95123 Catania, Italy;*
[2] *College of Physical Science and Technology, Sichuan University, Chengdu 610064, People's Republic of China.*

We compare two types of Tsallis distribution, i.e., with and without thermodynamical description, using the experimental data from the STAR, PHENIX, ALICE and CMS Collaborations on the rapidity and energy dependence of the transverse momentum spectra in p+p collisions. Both of them can give us the similar fitting power to the particle spectra. We show that the Tsallis distribution with thermodynamical description gives lower temperatures than the ones without it. The extra factor m_T (transverse mass) in the Tsallis distribution with thermodynamical description plays an important role in the discrepancies between the two types of Tsallis distribution. But for the heavy particles, the choice to use the m_T or E_T (transverse energy) in the Tsallis distribution becomes more crucial.

PACS numbers: 12.38.Mh, 24.60.Ak, 25.75.Ag

arXiv:1512.03555v1 [nucl-th] 11 Dec 2015

I. INTRODUCTION

The particle spectrum is a basic quantity directly measured in the experiments and it can reveal the information of particle production mechanism in heavy-ion collisions. Many physicists have devoted themselves to studying the particle spectra produced in the heavy-ion collisions using thermodynamical approaches, phenomenological methods, transport models *et al.* [1–22]. Recently, the Tsallis distribution, which was first proposed about twenty-seven years ago as a generalization of the Boltzmann-Gibbs distribution [23], has attracted many theorists' and experimentalists' attention in high energy heavy-ion collisions [5–9, 11–17, 24–33]. The excellent ability to fit the spectra of identified hadrons and charged particles in a large range of p_T up to 200 GeV, which covers 15 orders of magnitude, is quite impressive. This spectacular result was first shown by Wong *et al.* [14–17]. In refs. [21, 22], we have shown that Tsallis distribution can fit almost all the particle spectra produced in p+p, p+A and A+A at RHIC and LHC. From the phenomenological view, there may be real physics behind the prominently phenomenological work, e.g., Regge trajectory for particle classification [34]. We also note that there are different versions of Tsallis distribution in the literature and we classify them as Type-A, B and C to clarify the comparison in ref. [21]. Type-A Tsallis distribution is obtained without resorting to thermodynamical description, but it has been adopted to analyze the particle spectra by STAR [24], PHENIX [25] Collaborations at RHIC and ALICE [26–28], CMS [29] Collaborations at LHC. In ref. [21], we applied it to do the systematic analysis of identified particle spectra in p+p collisions at RHIC and LHC and proposed a cascade particle production mechanism. On the other hand, Type-B Tsallis distribution is derived by taking into account the thermodynamical consistency and is widely used by J. Cleymans and his collaborators to study the particle spectra in high-energy p+p collisions [8–10]. It is also used by the other authors [11]. Type-A and B are the most popular Tsallis distributions in the literature but they give quite different temperatures while fitting the same particle spectra, e.g., for pion, Type-A gives $T \sim 0.13$ GeV while Type-B gives $T \sim 0.075$ GeV. In this paper, we would like to systematically address the question what results in the discrepancies of the temperatures for the two types of Tsallis distribution using particle spectra in p+p collisions. The data produced in p+p collisions with different p_T ranges and different rapidity cuts are collected from the experimental Collaborations at RHIC and LHC [25–27, 30, 35–41].

The paper is organized as follows. In Sec. II, we introduce the two types of Tsallis distribution without and with thermodynamical description in our comparison. In order to make our discussion clear, we also introduce another three transient distributions which are very similar to Type-A and Type-B Tsallis distributions. In Sec. III, the results of particle spectra from the different distributions in p+p collisions and the comparisons are shown. A brief conclusion is given in the Sec. IV.

* Email address: zheng@lns.infn.it
† Email address: zhulilin@scu.edu.cn

II. TSALLIS DISTRIBUTIONS

Type-A Tsallis distribution has been widely adopted by STAR [24], PHENIX [25] Collaborations at RHIC and ALICE [26–28], CMS [29] Collaborations at LHC

$$E\frac{d^3N}{dp^3} = \frac{dN}{dy}\frac{(n-1)(n-2)}{2\pi nC[nC+m(n-2)]}(1+\frac{m_T-m}{nC})^{-n}, \tag{1}$$

where $m_T = \sqrt{p_T^2+m^2}$ is the transverse mass. m was used as a fitting parameter in ref. [24], but it represents the rest mass of the particle studied in refs. [25–29]. $\frac{dN}{dy}$, n and C are fitting parameters. When $p_T \gg m$, we can ignore the m in the last term in Eq. (1) and obtain $E\frac{d^3N}{dp^3} \propto p_T^{-n}$. This result is well known because high energy particles come from hard scattering and they follow a power law distribution with p_T. When $p_T \ll m$ which is the non-relativistic limit, we obtain $m_T - m = \frac{p_T^2}{2m} = E_T^{classical}$ and $E\frac{d^3N}{dp^3} \propto e^{-\frac{E_T^{classical}}{C}}$, i.e., a thermal distribution. The parameter C in Eq. (1) plays the same role as temperature T. In refs. [21, 22], we have obtained the simpler form of Eq. (1)

$$(E\frac{d^3N}{dp^3})_{|\eta|<a} = A(1+\frac{E_T}{nT})^{-n}, \tag{2}$$

where $E_T = m_T - m$. A, n and T are free fitting parameters in Eq. (2). We note that it has been used by CMS Collaboration [31, 32, 42] and by Wong *et al.* in their recent paper [16]. The STAR Collaboration also applied a formula which is very close to Eq. (2) [43]. We adopt the Eq. (2) in the following study.

In the framework of Tsallis statistics, the distribution function is

$$f(E,q) = [1+(q-1)\frac{E-\mu}{T}]^{-\frac{1}{q-1}}. \tag{3}$$

Taking into account the self-consistent thermodynamical description, one has to use the effective distribution $[f(E,q)]^q$. Therefore, the Tsallis distribution is obtained [8, 9, 11, 12]

$$E\frac{d^3N}{dp^3} = gV\frac{m_T\cosh y}{(2\pi)^3}[1+(q-1)\frac{m_T\cosh y-\mu}{T}]^{-\frac{q}{q-1}}, \tag{4}$$

where g is the degeneracy of the particle, V is the volume, y is the rapidity, μ is the chemical potential, T is the temperature and q is the entropic factor, which measures the non-additivity of the entropy. We dubbed it as the Type-B Tsallis distribution [21]. In Eq. (4), there are four parameters V, μ, T, q. μ was assumed to be 0 in refs. [8, 9, 11] which is a reasonable assumption because the energy is high enough and the chemical potential is much smaller than the temperature. In the mid-rapidity $y = 0$ region, Eq. (4) is reduced to

$$E\frac{d^3N}{dp^3} = gV\frac{m_T}{(2\pi)^3}[1+(q-1)\frac{m_T}{T}]^{-q/(q-1)}. \tag{5}$$

It becomes very similar to Eq. (2), but there are some differences, e.g., m_T replaces E_T in the bracket and there is an extra term m_T in front of the bracket. It should be pointed out that there is no direct match between n and q in Eqs. (2, 5). But we could find a connection between n and q in the limit at large p_T. When $p_T \gg m$, from Eq. (5), we can obtain

$$E\frac{d^3N}{dp^3} \propto p_T^{-\frac{1}{q-1}}. \tag{6}$$

Recalling that $E\frac{d^3N}{dp^3} \propto p_T^{-n}$ when $p_T \gg m$ from Eq. (1), therefore the relation between n and q is

$$n = \frac{1}{q-1}. \tag{7}$$

Another treatment to find the relation between n and q can be found in ref. [10].

For the other Tsallis distributions in the literature, we refer them to refs. [21, 22]. We noted that Type-A and Type-B Tsallis distributions can reproduce the particle spectra in p+p collisions very well but Type-B gives lower temperatures than the ones given by Type-A. In this paper, we would like to address this discrepancies between

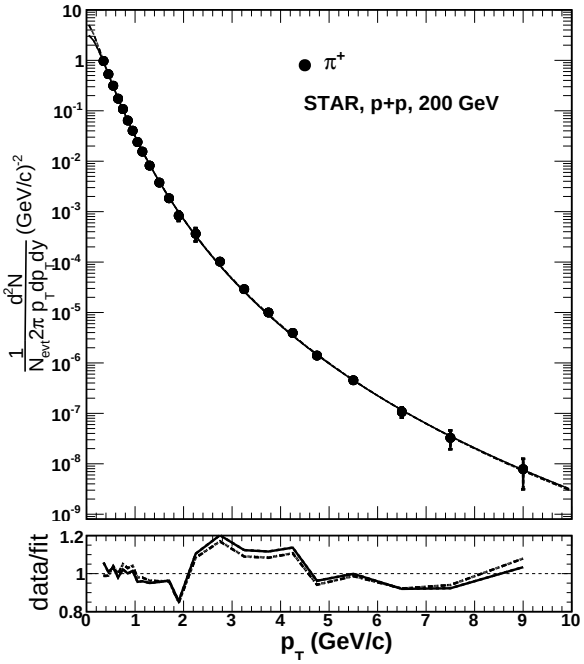

Figure 1: Fitting results using the distributions Eqs. (5, 8, 9, 10, 2) for π^+ in p+p collisions at $\sqrt{s}$ = 200 GeV. The solid line, dashed line, dotted line, dash-dotted line and long dash-dotted line refer to Eqs. (5, 8, 9, 10, 2) respectively, but they are hardly to distinguish because they give us similar fitting power. The ratios of data/fit are shown at the bottom. Data are taken from STAR [38].

the two types of Tsallis distribution. To make our discussion clear, another three transient distributions are used to bridge the Type-A and Type-B distributions. In ref. [44], a Tsallis-like distribution is obtained in the framework of non-extensive statistics for the particle invariant yield at midrapidity

$$E\frac{d^3N}{dp^3} = Am_T[1+(q-1)\frac{m_T}{T}]^{-\frac{1}{q-1}}, \tag{8}$$

where A, q and T are fitting parameters. Comparing Eq. (8) and Eq. (5), the only difference is the power of the distribution function, i.e., q for Eq. (5) and 1 for Eq. (8). We also introduce another two forms of distribution. One is

$$E\frac{d^3N}{dp^3} = A[1+(q-1)\frac{m_T}{T}]^{-\frac{q}{q-1}}, \tag{9}$$

where we neglect the term m_T outside of the bracket in Eq. (5) and the constants are absorbed into the parameter A. The other one is

$$E\frac{d^3N}{dp^3} = A[1+(q-1)\frac{m_T}{T}]^{-\frac{1}{q-1}}. \tag{10}$$

Similar to Eq. (9), we neglect the term m_T in front of the bracket in Eq. (8) but keep the rest. Using the relation Eq. (7), we find that Eq. (9) becomes Eq. (2) in the limit of massless particle.

Let us put the four distributions in order of Eqs. (5, 8, 10, 2) and Eqs. (5, 9, 10, 2), one can see that any adjacent distributions have only one term different. We successfully bridge the Type-A and Type-B Tsallis distributions and are able to conduct our investigation. We need to point out that even though we use the same symbols for the parameters in the five distributions, they may have different values when fitting the experimental data. In next section, we will systematically apply the five distributions to the particle spectra in p+p collisions, similar to our previous work [21]. But we update some experimental data which have larger p_T ranges and will focus on the temperature differences among the five distributions.

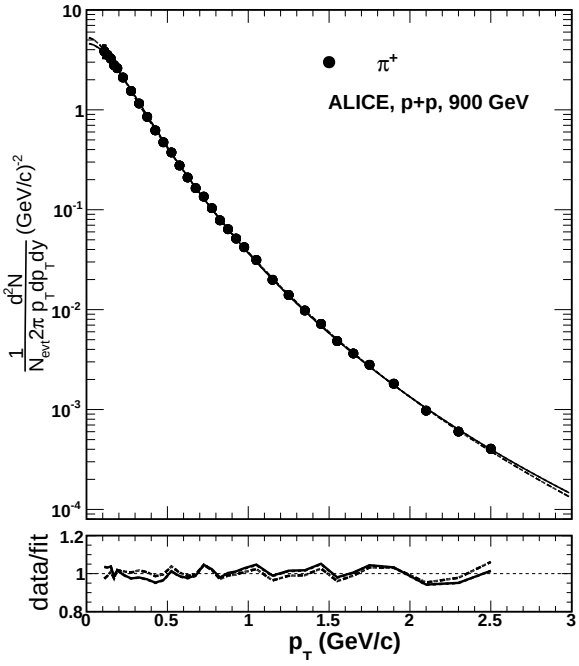

Figure 2: Same as in Fig. 1 for π^+ in p+p collisions at $\sqrt{s} = 900$ GeV. Data are taken from ALICE [27].

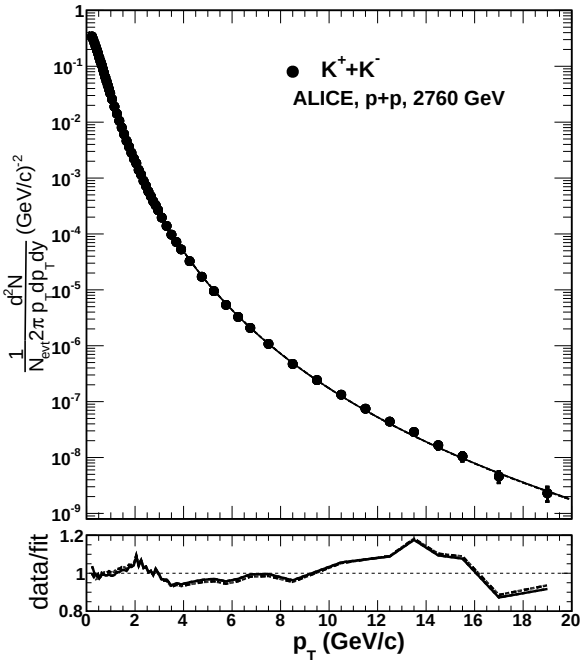

Figure 3: Same as in Fig. 1 for $K^+ + K^-$ in p+p collisions at $\sqrt{s} = 2760$ GeV. Data are taken from ALICE [35].

III. RESULTS

We fit the particle spectra with different p_T ranges and different rapidity cuts from p+p collisions at $\sqrt{s} = 62.4, 200, 900, 2760$ and 7000 GeV with the five distributions discussed in the last section. The fitting process is the same as that in refs. [21, 22]. Compared with ref. [21], the identified particle spectra data at $\sqrt{s} = 2760$ and 7000 GeV have been updated.

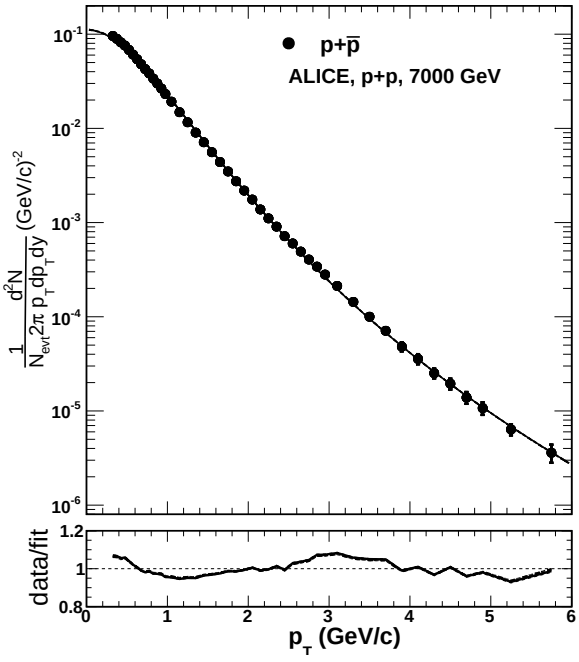

Figure 4: Same as in Fig. 1 for $p+\bar{p}$ in p+p collisions at $\sqrt{s}=7000$ GeV. Data are taken from ALICE [41].

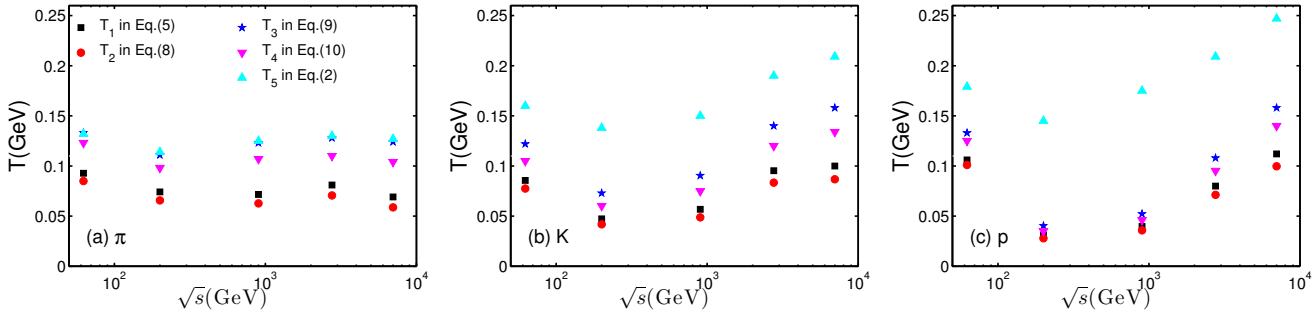

Figure 5: (Color online) Temperature T in the five distributions versus $\sqrt{s}$ for (a) π, (b) K and (c) p in p+p collisions.

In this work, we are interested in the differences of the parameter T from the five distributions. As we argued in refs. [21, 22], T is one free fitting parameter and can be different for different particles even they are produced in the same colliding system. In order to distinguish the parameter T in the five distributions and make our discussion clear, we assign T_1, T_2, T_3, T_4 and T_5 to Eqs. (5), (8), (9), (10) and (2), respectively. All the five distributions can fit the particle transverse momentum spectra very well. The values of T_i $(i=1,2,3,4,5)$ and corresponding χ^2_i/ndf for π, K, p and charged particles are shown in TABLE I. Here, we only show the fitting results with the five distributions for four cases: (1) π^+ at $\sqrt{s}=200$ GeV, (2) π^+ at $\sqrt{s}=900$ GeV, (3) K^++K^- at $\sqrt{s}=2760$ GeV, (4) $p+\bar{p}$ at $\sqrt{s}=7000$ GeV.

In Figs. 1 and 2, we show the fitting results for π^+ at $\sqrt{s}=200$ GeV from STAR Collaboration and $\sqrt{s}=900$ GeV from ALICE Collaboration using the five distributions Eq. (5) (solid line), Eq. (8) (dashed line), Eq. (9) (dotted line), Eq. (10) (dash-dotted line) and Eq. (2) (long dash-dotted line), respectively. Since the lines are so close to each other, they are almost indistinguishable in the figures. To visualize the fitting quality better, we also plot the ratios of experimental data and fitting results at the bottom of the figures. We can see that the five distributions can describe the experimentally measured π^+ transverse momentum spectra very well. The errors are within 20%.

To show the fitting results other than pions, we select the K^++K^- at $\sqrt{s}=2760$ GeV and $p+\bar{p}$ at $\sqrt{s}=7000$ GeV at LHC in Figs. 3 and 4, respectively. For the five distributions, we can not distinguish them at all in the two cases. Similar to pions, the fitting qualities are also very good.

From the above results, we can see that the five distributions have the same fitting power to the particle spectra. But

Table I: The fitting parameter T and corresponding χ^2/ndf in the distributions, Eqs. (5, 8, 9, 10, 2), for the particle spectra in p+p collisions. The unit of T is GeV.

data source	$\sqrt{s}$(GeV)	particle	T_1	χ^2_1/ndf	T_2	χ^2_2/ndf	T_3	χ^2_3/ndf	T_4	χ^2_4/ndf	T_5	χ^2_5/ndf
PHENIX[36]	62.4	π^0	0.104	1.433/11	0.097	1.451/11	0.136	1.663/11	0.126	1.656/11	0.135	1.686/11
PHENIX[25]	62.4	π^+	0.0927	6.857/23	0.085	6.866/23	0.133	4.767/23	0.123	4.784/23	0.132	4.779/23
		π^-	0.0898	8.049/23	0.0824	8.045/23	0.128	5.173/23	0.118	5.198/23	0.130	5.194/23
		K^+	0.0856	4.837/13	0.0775	4.822/13	0.122	5.141/13	0.105	5.349/13	0.160	5.121/13
		K^-	0.0936	2.002/13	0.0851	2.006/13	0.130	2.199/13	0.119	2.203/13	0.163	2.186/13
		p	0.106	7.017/ 24	0.101	7.075/24	0.133	6.934/24	0.125	6.945/24	0.179	6.966/24
		$\bar{p}$	0.0635	6.605/22	0.0588	6.563/22	0.0831	6.037/22	0.0817	5.079/22	0.148	7.178/22
PHENIX[37]	200	π^0	0.0873	18.396/22	0.0787	18.386/22	0.117	22.004/22	0.105	22.946/22	0.118	23.025/22
PHENIX[25]	200	π^+	0.0741	5.278/24	0.0657	5.275/24	0.111	4.491/24	0.0981	4.515/24	0.114	4.485/24
		π^-	0.0811	4.710/24	0.0725	4.703/24	0.121	3.350/24	0.108	3.372/24	0.123	3.354/24
		K^+	0.0473	1.561/13	0.0418	1.591/13	0.0729	1.634/13	0.0601	1.602/13	0.138	1.587/13
		K^-	0.0621	3.013/13	0.0542	3.010/13	0.0913	3.004/13	0.0781	2.999/13	0.147	2.999/13
		p	0.0311	23.832/31	0.0279	23.659/31	0.0404	24.004/31	0.0350	24.272/31	0.145	24.581/31
		$\bar{p}$	0.0473	12.902/31	0.0426	12.970/31	0.0609	13.240/31	0.0547	13.153/31	0.154	13.535/31
STAR[38]	200	π^+	0.0895	6.545/20	0.0809	6.539/20	0.126	5.032/20	0.113	5.008/20	0.128	5.009/20
		π^-	0.0900	6.855/20	0.0814	6.854/20	0.127	4.700/20	0.114	4.718/20	0.128	4.705/20
		p	0.0804	10.683/17	0.0735	10.653/17	0.104	10.375/17	0.0950	10.396	0.180	10.359/17
		$\bar{p}$	0.0765	10.380/17	0.0695	10.318/17	0.0995	10.079/17	0.0901	10.076/17	0.177	9.991/17
ALICE[26]	900	π^0	0.0922	7.991/10	0.0816	8.041/10	0.136	7.554/10	0.119	7.551/10	0.137	7.537/10
ALICE[27]	900	π^+	0.0716	24.640/30	0.0627	25.530/30	0.123	13.528/30	0.107	13.749/30	0.125	13.460/30
		π^-	0.0727	17.138/30	0.0636	17.602/30	0.125	12.394/30	0.109	12.645/30	0.126	12.483/30
		K^+	0.0568	12.790/24	0.0488	12.807/24	0.0904	13.034/24	0.0749	13.069/24	0.159	12.980/24
		K^-	0.0624	6.457/24	0.0538	6.552/24	0.0968	6.641/24	0.0820	6.636/24	0.161	6.609/24
		p	0.0397	13.879/21	0.0358	13.908/21	0.0522	13.816/21	0.0460	13.849/21	0.175	13.974/21
		$\bar{p}$	0.0649	13.586/21	0.0568	13.674/21	0.119	14.860/21	0.0769	13.544/21	0.188	13.675/21
ALICE[40]	2760	π^0	0.0951	6.164/15	0.0835	6.162/15	0.141	5.981/15	0.122	5.979/15	0.142	5.987/15
ALICE[35]	2760	$\pi^+ + \pi^-$	0.0810	149.545/ 60	0.0706	149.71/60	0.128	31.492/60	0.110	31.583/60	0.130	31.583/60
		$K^+ + K^-$	0.0953	10.339/55	0.0834	10.347/55	0.140	14.654/55	0.120	14.655/55	0.190	14.481/55
		$p + \bar{p}$	0.080	30.413/46	0.0712	30.647/46	0.108	33.068/46	0.0952	32.652/46	0.209	32.877/46
ALICE[26]	7000	π^0	0.0942	11.071/30	0.0822	11.112/30	0.142	16.664/30	0.122	16.707/30	0.142	16.750/30
ALICE[41]	7000	$\pi^+ + \pi^-$	0.0691	68.408/38	0.0587	68.193/38	0.124	26.041/38	0.104	26.539/38	0.127	26.216/38
		$K^+ + K^-$	0.100	7.807/45	0.0867	7.910/45	0.158	5.335/45	0.134	5.373/45	0.209	5.333/45
		$p + \bar{p}$	0.112	14.906/43	0.0997	14.763/43	0.158	12.719/43	0.140	12.684/43	0.247	12.700/43
CMS[30]	900	charged	0.0899	63.863/17	0.0794	63.940/17	0.127	85.844/17	0.110	85.2927/17	0.129	84.867/17
CMS[39]	2760	charged	0.0937	83.860/19	0.0818	84.026/19	0.135	110.614/19	0.115	110.770/19	0.136	110.4/19
CMS[30]	7000	charged	0.101	64.009/24	0.0880	63.955/24	0.148	80.316/24	0.126	80.353/24	0.147	80.25/24

as we can see from TABLE. I, the parameter T_i are different. It is the main purpose of this work to target what causes the temperature discrepancies among different Tsallis distributions, with and without thermodynamical description. In order to avoid confusion, we emphasis the meaning of each T_i. Using the Tsallis distribution classification in ref. [21], T_1 refers to Type-B Tsallis distribution and T_5 refers to Type-A Tsallis distribution. T_2, T_3 and T_4 are from the transient distributions to bridge the Type-A and Type-B Tsallis distributions. To have a clear picture for the parameter T_i from the five distributions, we plot T_i versus the colliding energy $\sqrt{s}$ for π, K and p, as shown in Fig. 5. We can clearly see that the Type-B Tsallis distribution gives lower T than the Type-A Tsallis distribution, as we mentioned in ref. [21]. For all the particles, T_1 and T_2 which are from the distributions, Eqs. (5, 8), with extra m_T term are lower than T_3, T_4 and T_5 which are from the distributions, Eqs. (9, 10, 2), without it. As we see that T_1 is larger than T_2, since Eq. (5) and Eq. (8) are similar except the power in the distributions, we conclude that the power q in Eq. (5) causes larger T. This can be verified by comparing T_3 with T_4. With the same argument, since T_4 is smaller than T_5, the m_T in Eq. (10) causes smaller T. To see the effects of q and m_T in the distribution, we can compare T_3 with T_5. For the light particles, i.e., pions (left panel), T_3 and T_5 are similar. The effects of the power q and m_T cancel each other. But for the heavier particles, i.e., kaons and protons (middle and right panels), the effect of m_T in Eq. (9) wins and T_3 is smaller than T_5. We note that the effect of the extra m_T term is crucial for the temperature difference between Type-A and Type-B Tsallis distributions, especially for the light particles. While for the heavier particles, the effect of the choice of m_T or E_T in the Tsallis distribution becomes more important as we

can see that T_5 is larger than the other T_i for kaons and protons in Fig. 5.

IV. SUMMARY

In this paper, we have presented a detailed investigation of two types of Tsallis distribution, with and without the thermodynamical description, by the p_T spectra measured from STAR, PHENIX Collaborations at RHIC and ALICE, CMS Collaborations at LHC. The power q in the Tsallis distribution with thermodynamical description is responsible for the thermodynamical consistency. To show a clear and complete comparison, another three transient distributions to bridge the two types of Tsallis distribution are also given. The five distributions have the similar fitting power to the particle spectra. The good agreements are obtained, but they give different temperatures. Agreed with our previous work [21], the Tsallis distribution with thermodynamical description gives lower T than the ones given by the distribution without it. The extra term m_T in the Tsallis distribution with thermodynamical description is responsible for the discrepancies of the temperatures. But for the heavier particles, the effect of the choice of m_T or E_T in the Tsallis distribution beats the effect of the extra term m_T. The data for p+p collisions at 8 and 13 TeV are coming. We wish these data would also support our conclusion presented here.

Conflict of Interests

The authors declare that there is no conflict of interests regarding the publication of this article.

Acknowledgments

We thank the anonymous referee who brought us to this topic. This work is supported by the NSFC of China under Grant No. 11205106.

[1] D. A. Teaney, "Viscous Hydrodynamics and the Quark Gluon Plasma", in *Quark-Gluon Plasma 4*, edited by R. C. Hwa and X.-N. Wang (World Scientific, Singapore, 2010), pp. 207-266.
[2] M. Gyulassy and X.-N. Wang, "Multiple collisions and induced gluon Bremsstrahlung in QCD ", Nuclear Physics B, vol. 420, pp. 583-614, 1994.
[3] R. C. Hwa and C. B. Yang, "Scaling behavior at high p_T and the p/π ratio", Physical Review C, vol. 67, Article ID 034902, 9 pages, 2003.
[4] V. Greco, C. M. Ko, and P. Lévai, "Parton coalescence and antiproton/pion anomaly at RHIC", Physical Review Letters, vol. 90, Article ID 202302, 4 pages, 2003.
[5] I. Sena and A. Deppman, "Systematic analysis of p_T-distributions in p+p collisions", The European Physical Journal A, vol. 49, Article ID 17, 5 pages, 2013.
[6] F. H. Liu, Y. Q. Gao and B. C. Li, "Comparing two-Boltzmann distribution and Tsallis statistics of particle transverse momentums in collisions at LHC energies", The European Physical Journal A, vol. 50, Article ID 123, 11 pages, 2014.
[7] P. K. Khandai, P. Sett, P. Shukla and V. Singh, "System size dependence of hadron p_T spectra in p+p and Au+Au collisions at $\sqrt{S_{NN}} = 200$ GeV", Journal of Physics G: Nuclear and Particle Physics, vol. 41, Article ID 025105, 10 pages, 2014.
[8] J. Cleymans and D. Worku, "The Tsallis distribution in proton-proton collisions at $\sqrt{s} = 0.9$ TeV at the LHC", Journal of Physics G: Nuclear and Particle Physics, vol. 39, Article ID 025006, 12 pages, 2012.
[9] M. D. Azmi and J. Cleymans, "Transverse momentum distributions in proton-proton collisions at LHC energies and Tsallis thermodynamics", Journal of Physics G: Nuclear and Particle Physics, vol. 41, Article ID 065001, 10 pages, 2014.
[10] J. Cleymans, G.I. Lykasov, A.S. Parvan, A.S. Sorin, O.V. Teryaev and D. Worku, "Systematic properties of the Tsallis distribution: Energy dependence of parameters in high energy p-p collisions", Physics Letters B, vol. 723, pp. 351-354, 2013.
[11] B. C. Li, Y. Z. Wang and F. H. Liu, "Formulation of transverse mass distributions in Au-Au collisions at $\sqrt{s_{NN}}$=200 GeV/nucleon", Physics Letters B, vol. 725, pp. 352-356, 2013.
[12] M. Rybczyński and Z. Włodarczyk, "Tsallis statistics approach to the transverse momentum distributions in p-p collisions", The European Physical Journal C, vol. 74, Article ID 2785, 5 pages, 2014.
[13] P.K. Khandai, P. Sett, P. Shukla and V. Singh, "HADRON SPECTRA IN p + p COLLISIONS AT RHIC AND LHC ENERGIES", International Journal of Modern Physics A, vol. 28, no. 16, Article ID 1350066, 12 pages, 2013.
[14] C. Y. Wong and G. Wilk, "Tsallis fits to p_T spectra and multiple hard scattering in pp collisions at the LHC", Physical Review D, vol. 87, Article ID 114007, 19 pages, 2013.

[15] C. Y. Wong and G. Wilk, "Tsallis fits to p_T spectra for pp collisions at the LHC", Acta Physica Polonica B, vol.43, no. 11, pp. 2047-2054, 2012.

[16] C.Y. Wong, G. Wilk, L.J.L. Cirto and C. Tsallis, "From QCD-based hard-scattering to nonextensive statistical mechanical descriptions of transverse momentum spectra in high-energy pp and $p\bar{p}$ collisions", Physical Review D, vol. 91, Article ID 114027, 16 pages, 2015.

[17] G. Wilk and Z. Włodarczyk, "Quasi-power laws in multiparticle production processes", Chaos, Solitons and Fractals, vol. 81, pp. 487-496, 2015.

[18] C. Beck, "Non-extensive statistical mechanics and particle spectra in elementary interactions", Physica A, vol. 286, pp. 164-180, 2000.

[19] I. Bautista, C. Pajares and J. Dias de Deus, "Evolution of particle density in high-energy pp collisions", Nuclear Physics A, vol. 882, pp. 44-48, 2012.

[20] L. L. Zhu, H. Zheng, and C. B. Yang, "Scaling behavior of transverse kinetic energy distributions in Au + Au collisions at $\sqrt{s_{NN}}$ = 200 GeV", Nuclear Physics A, vol. 802, pp. 122-130, 2008.

[21] H. Zheng, Lilin Zhu and A. Bonasera, "Systematic analysis of hadron spectra in p+p collisions using Tsallis distributions", Physical Review D, vol. 92, Article ID 074009, 7 pages, 2015.

[22] H. Zheng and Lilin Zhu, "Can Tsallis distribution fit all the particle spectra produced at RHIC and LHC?", Advances in High Energy Physics, vol. 2015, Article ID 180491, 9 pages, 2015.

[23] C. Tsallis, "Possible Generalization of Boltzmann-Gibbs Statistics", Journal of Statistical Physics, vol. 52, pp. 479-487, 1988.

[24] B. I. Abelev *et. al.* (STAR Collaboration), "Strange particle production in p + p collisions at $\sqrt{s}$= 200 GeV", Physical Review C, vol. 75, Article ID 064901, 21 pages, 2007.

[25] A. Adare *et al.* (PHENIX Collaboration), "Identified charged hadron production in p + p collisions at $\sqrt{s}$ = 200 and 62.4 GeV", Physical Review C, vol. 83, Article ID 064903, 29 pages, 2011.

[26] B. Abelev *et al.* (ALICE Collaboration), "Neutral pion and η meson production in proton-proton collisions at $\sqrt{s}$ = 0.9 TeV and $\sqrt{s}$ = 7 TeV", Physics Letters B, vol. 717, pp. 162-172, 2012.

[27] K. Aamodt *et al.* (ALICE Collaboration), "Production of pions, kaons and protons in pp collisions at $\sqrt{s}$ = 900 GeV with ALICE at the LHC", The European Physical Journal C, vol. 71, Article ID 1655, 22 pages, 2011.

[28] B. Abelev *et al.* (ALICE Collaboration), "Multi-strange baryon production in pp collisions at $\sqrt{s}$ = 7 TeV with ALICE", Physics Letters B, vol. 712, pp. 309-318, 2012.

[29] S. Chatrchyan *et al.* (CMS Collaboration), "Study of the inclusive production of charged pions, kaons, and protons in pp collisions at $\sqrt{s}$ = 0.9, 2.76, and 7 TeV", The European Physical Journal C, vol. 72, Article ID 2164, 37 pages, 2012.

[30] S. Chatrchyan *et al.* (CMS Collaboration), "Charged particle transverse momentum spectra in pp collisions at $\sqrt{s}$ = 0.9 and 7 TeV", Journal of High Energy Physics, vol. 2011, Issue 08, Article ID 086, 38 pages, 2011.

[31] V. Khachatryan *et al.* (CMS Collaboraction), "Transverse-momentum and pseudorapidity distributions of charged hadrons in pp collisions at $\sqrt{s}$ = 0.9 and 2.36 TeV", Journal of High Energy Physics, vol. 2010, Issue 02, Article ID 041, 19 pages, 2010.

[32] V. Khachatryan *et al.* (CMS Collaboraction), "Transverse-Momentum and Pseudorapidity Distributions of Charged Hadrons in pp Collisions at $\sqrt{s}$ = 7 TeV", Physical Review Letters, vol. 105, Article ID 022002, 14 pages, 2010.

[33] S. Chatrchyan *et al.* (CMS Collaboration), "Study of the production of charged pions, kaons, and protons in pPb collisions at $\sqrt{s_{NN}}$= 5.02TeV", The European Physical Journal C, vol. 74, Article ID 2847, 27 pages, 2014.

[34] C.Y. Wong, *Introduction to High-Energy Heavy-Ion Collisions,* (World Scientific, Singapore, 1994)

[35] B. Abelev *et al.* (ALICE Collaboration), "Production of charged pions, kaons and protons at large transverse momenta in pp and Pb-Pb collisions at $\sqrt{s_{NN}}$ = 2.76 TeV", Physics Letters B, vol. 736, pp. 196-207, 2014.

[36] A. Adare *et al.* (PHENIX Collaboration), "Inclusive cross section and double helicity asymmetry for π^0 production in p+p collisions at $\sqrt{s}$ = 62.4 GeV", Physical Review D, vol. 79, Article ID 012003, 11 pages, 2009.

[37] A. Adare *et al.* (PHENIX Collaboration), "Inclusive cross section and double helicity asymmetry for π^0 production in p+p collisions at $\sqrt{s}$=200 GeV: Implications for the polarized gluon distribution in the proton", Physical Review D, vol. 76, Article ID 051106(R), 7 pages, 2007.

[38] J. Adams *et al.* (STAR Collaboration), "Identified hadron spectra at large transverse momentum in p+p and d+Au collisions at $\sqrt{s_{NN}}$ = 200 GeV", Physics Letters B, vol. 637, pp. 161-169, 2006.

[39] S. Chatrchyan *et al.* (CMS Collaboration), "Study of high-p_T charged particle suppression in PbPb compared to pp collisions at $\sqrt{s_{NN}}$=2.76 TeV", The European Physical Journal C, vol. 72, Article ID 1945, 22 pages, 2012.

[40] B. Abelev *et al.* (ALICE Collaboration), "Neutral pion production at midrapidity in pp and Pb-Pb collisions at $\sqrt{s_{NN}}$ = 2.76 TeV", The European Physical Journal C, vol. 74, Article ID 3108, 20 pages, 2014.

[41] J. Adam *et al.* (ALICE Collaboration), "Measurement of pion, kaon and proton production in proton-proton collisions at $\sqrt{s}$ = 7 TeV", The European Physical Journal C, vol. 75, Article ID 226, 23 pages, 2015.

[42] S. Chatrchyan *et al.* (CMS Collaboration), "Measurement of the Λ_b cross section and the $\bar{\Lambda}_b$ to Λ_b ratio with $J/\psi\Lambda$ decays in pp collisions at $\sqrt{s}$ = 7 TeV", Physics Letters B, vol. 714, pp. 136-157, 2012.

[43] B. I. Abelev *et al.* (STAR Collaboration), "Inclusive π^0, η, and direct photon production at high transverse momentum in p + p and d + Au collisions at $\sqrt{s_{NN}}$ = 200 GeV", Physical Review C, vol. 81, Article ID 064904, 26 pages, 2010.

[44] W.M. Alberico and A. Lavagno, "Non-extensive statistical effects in high-energy collisions", The European Physical Journal A, vol. 40, pp. 313-323, 2009.